### Title

Experimental study of a direct evaporative cooling approach for Li-ion battery thermal management




### Journal

International Journal of Energy Research, 44(8)

### ISSN

0363-907X



### Authors

Zhao, Rui
Liu, Jie
Gu, Junjie
et al.



### Publication Date

2020-06-25

### DOI

10.1002/er.5402

Peer reviewed

Received: 19 December 2019 | Revised: 10 March 2020 | Accepted: 17 March 2020

DOI: 10.1002/er.5402



RESEARCH ARTICLE

INTERNATIONAL JOURNAL OF ENERGY RESEARCH WILEY

# Experimental study of a direct evaporative cooling approach for Li-ion battery thermal management

**Rui Zhao**[1,2] | **Jie Liu**[1,3] | **Junjie Gu**[3] | **Long Zhai**[3] | **Fai Ma**[2]

[1]National Research Base of Intelligent Manufacturing Service, Chongqing Technology and Business University, Chongqing, China

[2]Department of Mechanical Engineering, University of California, Berkeley, California

[3]Department of Mechanical and Aerospace Engineering, Carleton University, Ottawa, Ontario, Canada

**Correspondence**
Jie Liu, Department of Mechanical and Aerospace Engineering, Carleton University, Ottawa, ON, Canada.
Email: jie.liu@carleton.ca

**Funding information**
Chongqing Technology and Business University, Grant/Award Number: KFJJ2016034; National Sciences and Engineering Research Council Canada

**Summary**

A desirable operating temperature range and small temperature gradient is beneficial to the safety and longevity of lithium-ion (Li-ion) batteries, and battery thermal management systems (BTMSs) play a critical role in achieving the temperature control. Having the advantages of direct access and low viscosity, air is widely used as a cooling medium in BTMSs. In this paper, an air-based BTMS is modified by integrating a direct evaporative cooling (DEC) system, which helps reduce the inlet air temperature for enhanced heat dissipation. Experiments are carried out on 18650-type batteries and a 9-cell battery pack to study how relative humidity and air flow rate affect the DEC system. The maximum temperatures, temperature differences, and capacity fading of batteries are compared between three cooling conditions, which include the proposed DEC, air cooling, and natural convection cooling. In addition, a DEC tunnel that can produce reciprocating air flow is assembled to further reduce the maximum temperature and temperature difference inside the battery pack. It is demonstrated that the proposed DEC system can expand the usage of Li-ion batteries in more adverse and intensive operating conditions.

**KEYWORDS**

air cooling, direct evaporative cooling, lithium-ion battery, reciprocating air flow, thermal management system

## 1 | INTRODUCTION

Lithium-ion (Li-ion) batteries have emerged as one of the most promising energy storage technologies for portable electronic devices, drones, electric vehicles, and residential and grid-scale energy storage due to their high specific energy, lightweight, no memory effect, and low self-discharge rate. Although offering many advantages and benefits, Li-ion batteries are delicate, and their degradation rate can soar as the operating temperature is outside the optimum range of 10°C to 60°C.[1,2] Battery thermal management systems (BTMSs) are essential for Li-ion batteries to operate within a desirable temperature range with minimal temperature changes, and thus to guarantee their efficiency, robustness, and safety.

BTMSs can be categorized into active and passive modes.[3,4] The active BTMSs circulate air or liquid through fans or pumps in cooling channels to extract the heat generated by batteries, while the passive BTMSs manage battery heat generation without consuming supplementary energy, and the examples include phase change materials cooling,[5-10] hydrogel cooling,[11-13] and boiling liquid cooling.[14-16] As the modern trend toward increasing batteries' power density and

**Abbreviation:** BTMS, battery thermal management system; DEC, direct evaporative cooling; EC, evaporative cooling; ECR, evaporative cooling with reciprocating air flow; RH, relative humidity; SPDT, single pole double throw.

  

fast charging performance, that is, higher C rates (for example, 2 C indicates the current that can fully charge or discharge a battery in 1/2 hour), the parasitic heat generation in batteries can increase, which poses extra challenges on the BTMSs. In this regard, an active BTMS becomes more suitable to meet this trend since it can continuously bring in cold medium for battery cooling.

Air cooling is one of the most commonly adopted approaches used in electronics cooling and battery pack cooling in electric vehicles. It has been well commercialized and extensively studied in literature due to the easy access of the air and the simple structure of the system, and the research on air-based BTMSs mainly falls into two categories, the optimizations of battery layout and flow path.[17-24] For example, cylindrical Li-ion battery pack with aligned and staggered cell arrangements has been numerically studied, in which the results showed that the aligned cell arrangement excels, with having higher cooling index and lower power consumption than the staggered layout.[23] In applications that require fixed cell layouts, redesign of cooling channels and flow paths as well as adding pressure relief ventilations can be considered to achieve a better cooling effect. For example, Sun and Dixon[25] compared the peak temperature and temperature difference of a prismatic battery pack cooled in U-type, Z-type, and tapered Z-type cooling configurations. A Z-type cooling channel with tapered upper and lower ducts can significantly reduce the maximum temperature and improve the temperature uniformity in the battery pack. A reciprocating air flow design was proposed and numerically analyzed in Reference 26. This design effectively eliminated the heat accumulation in the batteries that are close to the cooling tunnel exit, and therefore reduced the temperature differences in batteries.

Existing research on the air-based BTMSs mainly aims at improving the effective contact between cold air and hot batteries to enhance the heat dissipation, in which the intake air has the same temperature as the ambient air. Increased heat dissipation rates can be attained on the existing air-based BTMSs if the intake air temperature could become lower, and it will make the air cooling more robust for dealing with high-intensity charging/discharging scenarios, such as the batteries used in Formula E racing vehicles. Evaporative cooling is a mature technology that has been used in industrial cooling for decades, for instance in cooling towers and gas turbines.[27,28] It utilizes the evaporation of water from liquid to vapor to reduce the sensible heat of air via an isenthalpic process and lower its temperature, and a schematic illustration is given in Figure 1A. In Reference 29, Carmona explained the theory of the evaporative cooling in detail, and a case study was also performed on augmenting the power generation of a gas turbine generator through implementing the evaporative cooling. The evaporative cooling approach has seldom been reported for battery thermal management. In relevant studies, a heat pipe-based BTMS was combined with the evaporative cooling to manage the heat of prismatic battery packs, in which the heat generated from the batteries was indirectly absorbed by water evaporation through the assist of heat pipes.[30] In Reference 12, water filled hydrogel films were adhered to the surfaces of a prismatic battery pack to absorb the heat through the natural evaporation of water in the films.

In comparison, direct evaporative cooling (DEC) is simpler and more cost-effective than the indirect cooling methods given above, and it is achieved by forcing evaporation-cooled air directly to the cooling channels between batteries to dissipate the generated heat. To the best of our knowledge, the DEC has not been studied in literature for Li-ion battery thermal management. In this work, small-scale DEC tunnels are built to examine the cooling ability of the DEC approach, in which wick filters are assembled to regulate air flow and evaporate water for obtaining cooled inlet air. Cooling experiments are carried out on single batteries and battery packs using natural convection cooling, air cooling, and DEC for comparison. In addition, the DEC experiments are carried out all year round to target a range of humidity to study its effect on the evaporative cooling process. Comprehensive analyses of a psychrometric chart are also performed to investigate the cooling potential (CP) of the DEC system and its suitable application scenarios. Lastly, a reciprocating flow mode is integrated with the DEC tunnel to achieve a uniform temperature distribution.

## 2 | EXPERIMENTAL SETUP

The batteries used in the experiments are Panasonic NCR18650B cylindrical batteries, and their specifications are provided in Table 1. The battery pack consists of nine batteries that are electrically connected in series and immobilized by spacers, and the transversal and longitudinal distances between neighboring batteries are 2.5 mm.

Figure 1C shows the one-directional cooling tunnel, which has two levels: the 90 mm upper level is for battery and fan installations as well as air flow, while the 5 mm lower level is designed to store the extra water during evaporation. The baffle that separates the two levels is glued and sealed with the tunnel walls on its three edges, while the other edge is spaced 25 mm apart from the tunnel wall for wick filter installation. The single battery/battery pack for testing is placed in the center of the tunnel, and K-type thermocouple(s) is taped on the battery

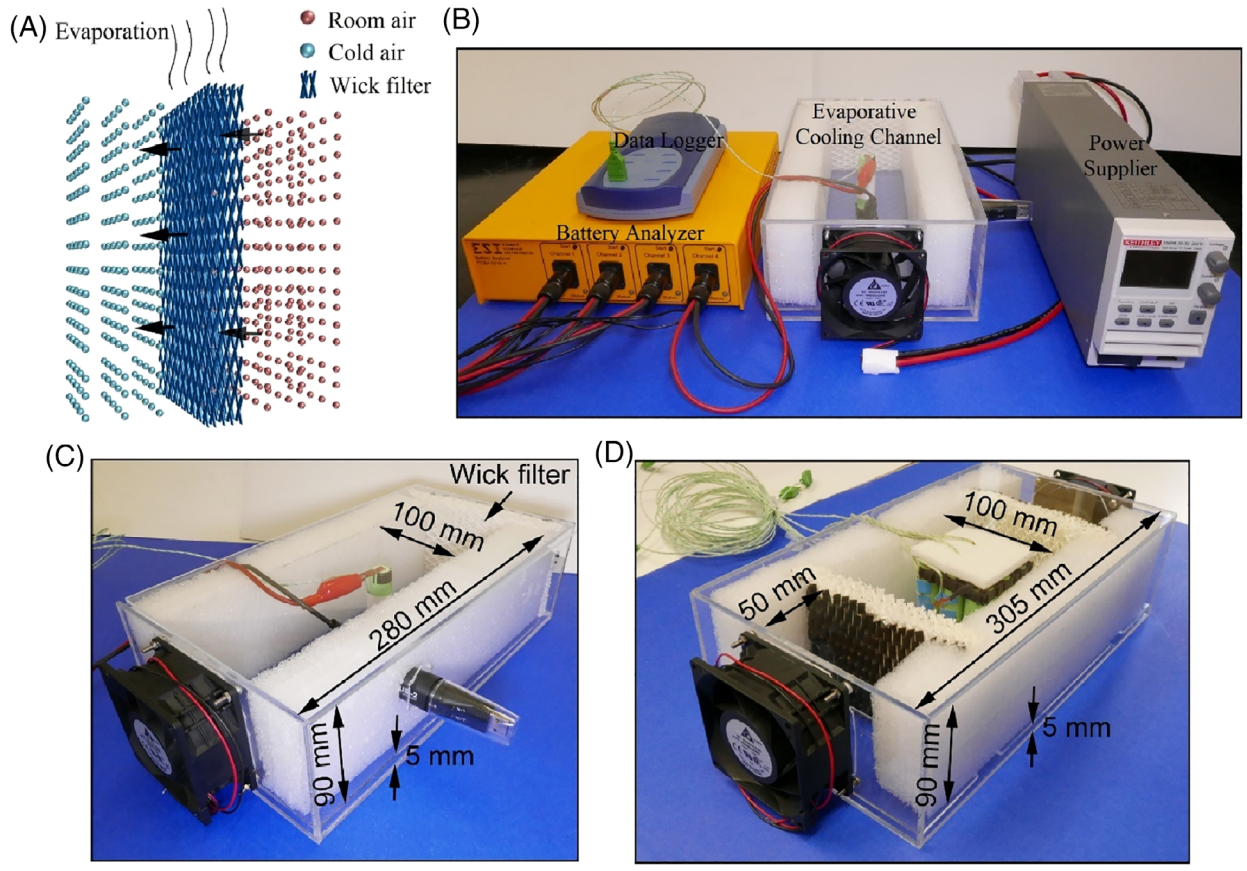


**FIGURE 1** Photos of the experimental setup. A, Schematic illustration of the DEC method. B, The experimental bench. C, The one-directional cooling tunnel. D, The DEC tunnel for providing reciprocating air flow [Colour figure can be viewed at wileyonlinelibrary.com]

**TABLE 1** Specifications of the Panasonic NCR18650B cylindrical battery

| | **Panasonic NCR18650B** |
|---|---|
| Diameter (mm) | 18.2 |
| Height (mm) | 65.0 |
| Weight (g) | 47.8 |
| Nominal voltage (V) | 3.6 |
| Nominal Capacity (mAh) | 3350 |
| Specific energy (W/kg) | 242 |
| Energy density (W/L) | 675 |
| Standard charging current (A) | 1.63 |
| Discharge temperature (°C) | −20 to 60 |
| Charge temperature (°C) | 0 to 45 |

surface(s) for temperature measurement, as shown in Figure 1C,D. The accuracy and resolution of the thermocouples are ±0.5°C and 0.025°C, respectively, and all thermocouples are calibrated in ice water prior to test. An EL-USB-2 humidity logger is also installed in the tunnel to record the relative humidity (RH), and it has an accuracy and resolution of 2.25% and 0.5%, respectively. The tunnel that can provide reciprocating air flow is shown in Figure 1D, which has a similar structure as the one-directional tunnel except using two sets of wick filters and fans. In practice, the reciprocating air flow can be attained by using flip door valves to reverse the air flow, which only needs one cooling fan and is more cost-effective.[26]

Three cooling systems including natural convection cooling (baseline), forced air cooling, and DEC are applied on the batteries during tests. In the baseline condition, the battery/battery pack is placed in the one-directional tunnel and connected to an ESI PCBA 5010-4 battery analyzer for charge/discharge, and the fan is in the off state during the entire tests. The temperature of the battery/battery pack is recorded during and after the discharging until it is stable and close to the ambient temperature.

The air cooling test is performed in the same way as the baseline case except the operation of the cooling fan that draws air through the tunnel. The cooling fans used

in this work are DC brushless fans from Delta Electronics (PFB0824DHE), and its specifications are given in Table 2. They are powered by a DC power supplier Keithley 2260B-30-36 at different power outputs, as shown in Figure 1B.

For the DEC, the wick filters are kept moisture during tests. Specifically, in the one-directional tunnel, the cooling fan draws the air out of the tunnel during the tests and the filter is refilled with 20 mL of water every 5 minutes. In the reciprocating tunnel, the power supplier and two fans are connected to a single pole double throw (SPDT) switch so they can blow out the air alternatively. Based on the reciprocating cooling research results published by Mahamud and Park,[26] the reciprocating period is set to 120 seconds for fan switches and water refills (10 mL water per refill). A schematic is also shown in Figure 2 for a clear illustration. Due to the symmetry, we only measured the surface temperatures of the batteries in the first two rows of the battery pack, as the locations 1 to 6 shown in Figure 2.

Cooling experiments including constant current (CC) discharges and cycles tests are carried out on the batteries equipped with the previously mentioned cooling systems. Batteries used in the tests are fresh and they are preconditioned under a constant rate of 0.5 C between 2.5 and 4.2 V for five cycles before testing. This procedure will eliminate the impact of solid electrolyte interface formation on the thermal behaviors of the batteries between cycles. Meanwhile, the batteries used in the battery pack are tested to ensure that they have similar capacities. The maximum capacity difference between batteries is within 50 mAh when discharged at 0.5 C.

Prior to the CC discharge test, the single batteries and the battery pack are fully charged to voltages of 4.2 and 37.8 V, respectively, at a CC of 1 A and a cut-off current of 0.05 A at the constant voltage (CV) stage. During the discharges, the current and cut-off voltage of the single batteries are set to 5 A and 2.6 V, respectively, and are 3 A or 5 A and 25 V for the battery pack.

zDuring the cycle test, vinyl tubing with drilled holes passes through the filter to continuously supply water for evaporation. The battery tested in the baseline condition is cycled between 3.0 and 4.2 V, and the batteries equipped with the DEC and air cooling systems are cycled between 2.5 and 4.2 V. The cycled batteries are charged (CC-CV) and discharged (CC) at the maximum tolerated currents of 3.35 A (1 C) and 6.7 A (2 C), respectively, for faster fading and a clear comparison of their capacity losses. A detailed explanation of the selection of the voltage ranges in the cycle test will be given in the Section 3.3.

**TABLE 2** Specifications of the cooling fan

| Parameters | Values |
|---|---|
| Diameter (mm) | 80 |
| Width (mm) | 32 |
| Weight (g) | 200 |
| Rated voltage (V) | 24 |
| Rated power (W) | 32.4 |
| Maximum air flow ($m^3$/min) | 3.75 |
| Maximum speed (rpm) | 9000 |
| Testing voltage (V) | 9, 12, and 15 |
| Testing current (A) | 0.33, 0.64, and 0.8 |
| Testing power (W) | 2.97, 7.68, and 12.0 |

## 3 | RESULTS AND DISCUSSION

### 3.1 | The effect of RH on DEC

In Figure 3A, the temperature curves of the cylindrical Li-ion battery during 5 A discharges are plotted under

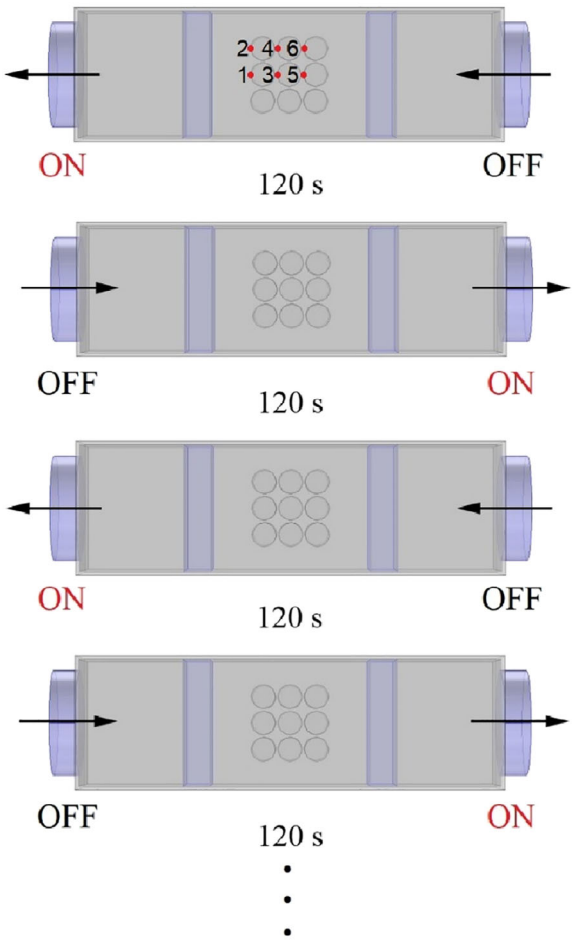


**FIGURE 2** Schematic illustration of the reciprocating air flow in a tunnel [Colour figure can be viewed at wileyonlinelibrary.com]

different cooling conditions. It is seen that for the baseline condition, the temperature of the battery increases during the discharge, and a maximum temperature of 59.1°C is reached at the end of discharge, which is significantly higher than that of the battery equipped with cooling systems. Consequently, the time spent for cooling the fully discharged battery from the peak temperature to room temperature (will be called "cooling time" in the following text) even reaches 4795 s due to the high temperature and low heat dissipation rate, which prevents the battery from operating seamlessly for the following cycles. For the air cooling and DEC, the fan operates at a

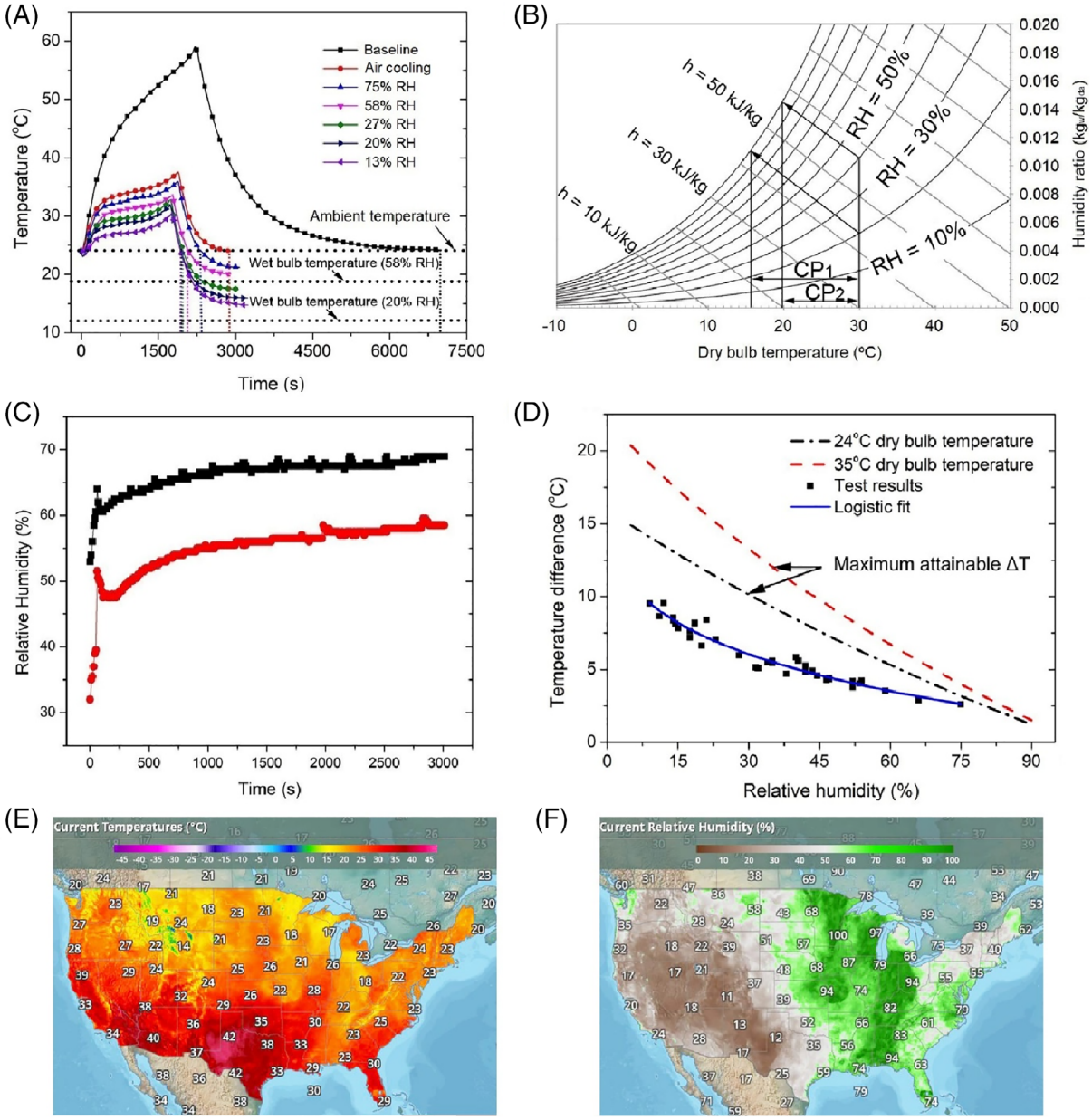


**FIGURE 3** Performance validation of the DEC approach for Li-ion battery thermal management. A, Comparisons of the surface temperatures of a Panasonic NCR18650B cylindrical battery during 5 A discharges under different cooling conditions, where the dot lines show the ambient temperature, wet bulb temperature at 58% RH, and wet bulb temperature at 20% RH. B, Psychrometric chat at 101.325 kPa, adapted from Ref. [29], used for illustrating the cooling capacity (CP) in two scenarios. C, The changes of the RH in the one-directional DEC tunnel during the tests at initial RH values of 32% (red circle) and 53% (black square). D, A scatter diagram and a logistic fit of the temperature differences between stabilized battery temperature and ambient temperature under different ambient RH levels, as well as plots of CP versus RH at ambient temperatures of 24°C and 35°C. E, The temperature map and F, RH map in the contiguous United States in the afternoon of August 26, 2019[31] [Colour figure can be viewed at wileyonlinelibrary.com]

power of 2.97 W, which is the minimum power to drive the fan motor. The use of a cooling fan can significantly improve the heat dissipation at the battery surface. It is seen that the temperature increases at a lower rate and the maximum temperature and cooling time drop to 37.6°C and 1048 seconds, respectively, when the ambient air is directly forced to cool the battery, as shown by the red curve with red circles.

The battery temperature profiles during the DEC are dependent on the ambient RH, and a better cooling performance can be achieved at a lower RH, as the temperature curves shown in Figure 3A. A psychrometric chart is provided in Figure 3B to explain this effect. The 30°C ambient air with initial RHs of 20% and 40%, for example, is compared in their CP, which is defined as the temperature difference between the dry bulb temperature and wet bulb temperature (the lowest attainable air temperature). It is seen that for the same temperature, the air with lower RH has more room to hold the evaporated vapor until it reaches the saturated state, thus having a higher CP than the high RH air, that is, $CP_1 > CP_2$. Figure 3A shows the DEC results at five selected RH conditions. It is seen that the proposed DEC outperforms the air cooling in managing the battery heat, and it becomes more evident for low RH conditions. As an example, at a RH of 13%, the battery discharged in the DEC tunnel has a temperature rise of 6.5°C (7.1°C lower than the air cooling) and a cooling time of 168 seconds (880 seconds quicker than the air cooling). Its excellence in thermal management is due to the low intake air temperature, which increases the heat dissipation rate, $\dot{Q}$, given as the basic relationship for heat transfer by convection:

$$\dot{Q} = hA\left(T_s - T_f\right) \tag{1}$$

where $h$ is the heat transfer coefficient, $A$ is the area of the object faced toward the cooling medium at a temperature of $T_f$, and $T_s$ is the surface temperature of the object. The test results shown in Figure 3A are also summarized in Table 3.

In Figure 3A, it is also seen that under different ambient RH levels, the battery temperature stabilizes at different values, and these temperatures are relatively higher than the corresponding wet bulb temperatures at 1 atm. As an example, the wet bulb temperature at RH values of 20% and 58% are plotted in dotted lines in Figure 3A, which are lower than the stabilized temperatures. This is because the air that passes through the wick filter is not fully saturated. As shown in Figure 3C, the RH in the tunnel stabilized at 58% and 69% when the initial RH values are 32% and 53%, respectively. In practice, the stabilized RH can be adjusted through using wick filters of different microstructures, since the water evaporation rate is related to the contact area between the air and the wick filter.[32]

**TABLE 3** Summary of the results from Figure 3A

| | Temperature rise (°C) | Cooling time (s) |
|---|---|---|
| Natural convection | 35.1 | 4795 |
| 9 V direct | 13.6 | 1048 |
| 9 V EC at 75% RH | 11.9 | 454 |
| 9 V EC at 58% RH | 9.5 | 306 |
| 9 V EC at 27% RH | 8.7 | 236 |
| 9 V EC at 20% RH | 7.9 | 211 |
| 9 V EC at 13% RH | 6.5 | 168 |

Abbreviations: EC, evaporative cooling; RH, relative humidity.

In experiments, a total of 40 DEC tests were carried out under different ambient RH levels, and the difference between the stabilized battery temperature and room temperature at the end of each test is taken and plotted against the corresponding ambient RH, as the scatter shown in Figure 3D, which shows a similar trend as the maximum attainable temperature drop (ie, CP) versus RH at an ambient temperature of 24°C, as the black dash dot line shown in Figure 3D. The maximum attainable temperature drop can be achieved when the air passing through the filter is fully saturated. To achieve better cooling, the future work may improve the wick filter to evaporate water at a faster rate but maintain the RH within the allowable range for battery operation. A logistic fit given by the following equation is also shown in Figure 3D to describe the relation between the temperature difference and ambient RH for this work.

$$\Delta T = -29.3 + \frac{45.8}{1 + \left(\frac{RH \times 100}{548}\right)^{0.419}} \tag{2}$$

where the unit of temperature is in Celsius, and the adjusted R-squared of the logistic fit of the experimental data is 0.95. When the RH of ambient air is known, it can be substituted into the logistic fit Equation (2) to calculate the attainable temperature drop of the ambient air.

It is noteworthy that in this work, all the tests were performed in a laboratory that is kept at 24°C. However, in many cities, the temperature in the middle or late afternoon can exceed 35°C during the summer, and the RH also reaches the lowest value in the afternoon, which makes the DEC more adequate for battery thermal management than air cooling. As the plot of the maximum temperature drop against RH shown in Figure 3D, the

DEC at 35°C shows higher CP than that at 24°C, especially for low RH conditions. As an example, the temperature and RH maps in the contiguous United States on an August afternoon are plotted in Figure 3E,F to illustrate the suitability of implementing the DEC system. It is observed that the west region of the United States is ideal for the implementation of the DEC due to its low RH and high temperature. Although low precipitation is anticipated in that region, the DEC is still an effective cooling option and it is worthy to do so if the cost of water is trivial compared to the cooling benefits, such as in formula E races.

## 3.2 | The effect of air flow rate on DEC

To study the effect of air flow rate on the cooling performance of the air cooling and DEC systems, the voltage input to the fan was increased from 9 to 12 V and 15 V to yield higher powers of 7.68 and 12.0 W. Three repeated tests were carried out for each cooling condition. The temperature curves and the temperature rise column charts (insets) of the battery discharged in the air cooling and DEC tunnels are shown in Figure 4A,B, respectively. With the air cooling system, the battery temperature increases at a lower rate as the power of cooling fan increases due to the higher convection heat transfer coefficient. As the inset in Figure 4A shown, 2.3°C and 3.8°C drops in the maximum temperature are obtained in the air cooling system as the power increases from 2.97 to 7.68 W and 12.0 W. Similar trend is also found in the DEC tunnel, where the drops of the temperature rises are 2.3°C and 4.0°C. From the comparison, it is economical to maintain the fan power at a relative lower level at which the batteries can operate safely and reliably, since the increased power input cannot further improve the performance of the DEC against the air cooling. The maximum temperature rises given in the insets of Figure 4A,B are the average values of three repeated tests in different cooling conditions. Small variations of the temperature rises are observed between tests, as the error bars indicated in the insets.

In Figure 4B, it is seen that at the early stage of discharges, the temperature of the battery cooled in the DEC tunnel experiences slight temperature drops due to the low intake air temperature that improves the convective heat dissipation. Small temperature fluctuations are also observed after each water refill. This is because the injection of room temperature water breaks the balance of evaporation and increase the inlet air temperature. It is also noteworthy that the peak temperature of the battery cooled in the DEC tunnel at a fan power of 2.97 W is even 1.8°C lower than that of the battery cooled by ambient air at a fan power of 12.0 W. It can be concluded that the DEC helps the battery system achieve the optimum cooling performance while ensuring the least amount of power consumption.

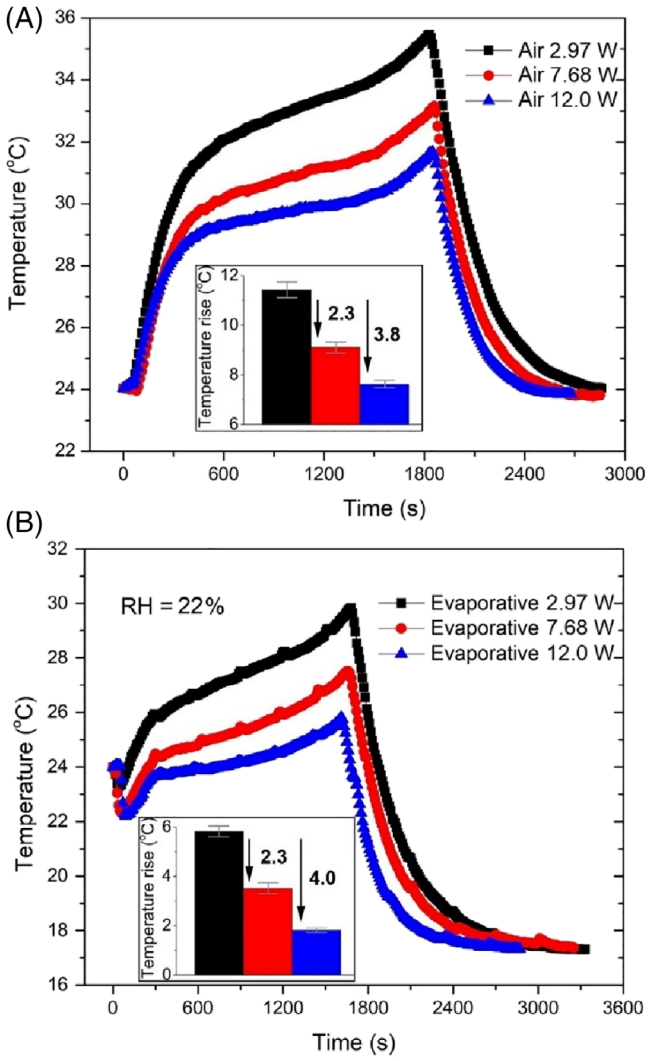


**FIGURE 4** Temperature curves and temperature rise charts of single batteries during 5 A discharges. A, In direct air cooling tunnel at different fan powers. B, In DEC tunnel at different fan powers [Colour figure can be viewed at wileyonlinelibrary.com]

## 3.3 | Cycle tests

In this section, the capacity fading of single batteries cycled in different cooling conditions is compared. Figure 5A,B show the voltage and temperature curves of the battery cycled between 2.5 and 4.2 V in the baseline condition. It is seen that the maximum battery temperature reaches 71°C at the end of discharging, which far exceeds the upper temperature limit of 60°C. The

temperature of the battery returns to its initial temperature after a 4-hour constant-current-constant-voltage charging process. To ensure the safety of the battery during the cycle test, the lower voltage limit was set to 3.0 V for the battery cycled in the baseline condition.

Figure 6A shows the charging and discharging voltages of the batteries cycled in different cooling conditions. After increasing the lower voltage limit of the battery cycled in the baseline condition from 2.5 to 3.0 V, the discharged capacity of the battery decreases from 3197 to 2447 mAh, which falls between the discharged capacities of the batteries with the DEC system (2419 mAh) and the air cooling system (2725 mAh). Therefore, the battery cycled in the adjusted voltage range is more adequate for comparison due to the similar levels of active material utilizations in anodes and cathodes compared to the other two batteries.

The comparison of the discharge curves in Figure 6A shows that the battery in the baseline condition has higher voltage plateau than that of the batteries in forced cooling conditions, and the battery cycled in the DEC has the biggest potential drop among the batteries. This is attributed to the fact that the flows of ions and electrons are easier at high temperatures. Figure 6A shows the temperature profiles of the batteries cycled in the three cooling conditions. It is seen that all of the three batteries can restore to their initial temperature after each cycle due to the long constant-voltage charging stage. Flat temperature plateaus are also seen at end of the CC charging

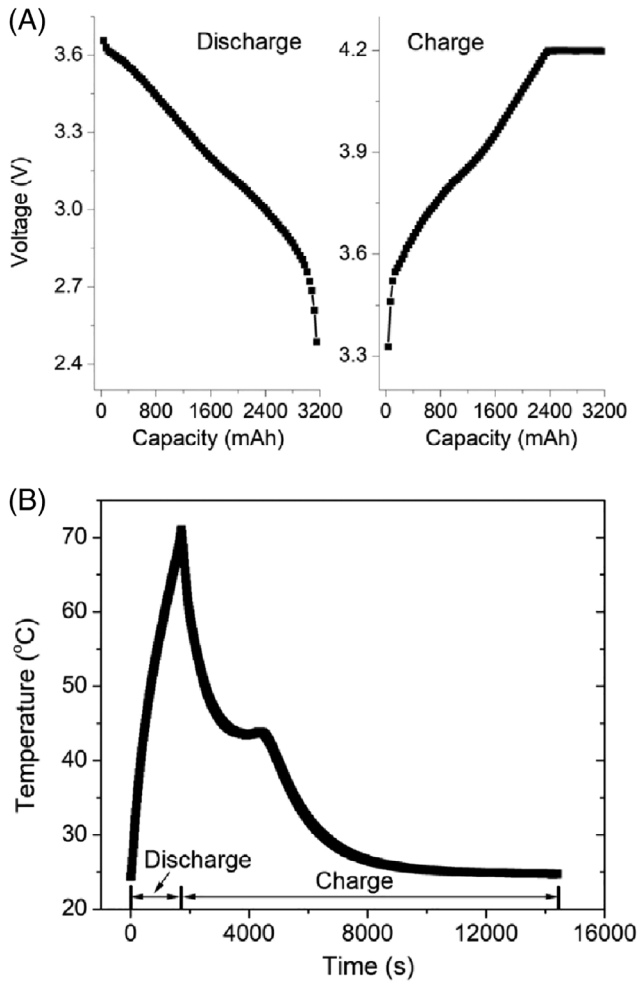


**FIGURE 5** A, Voltage and B, temperature curves of the battery cycled between 2.5 V and 4.2 V in the baseline condition

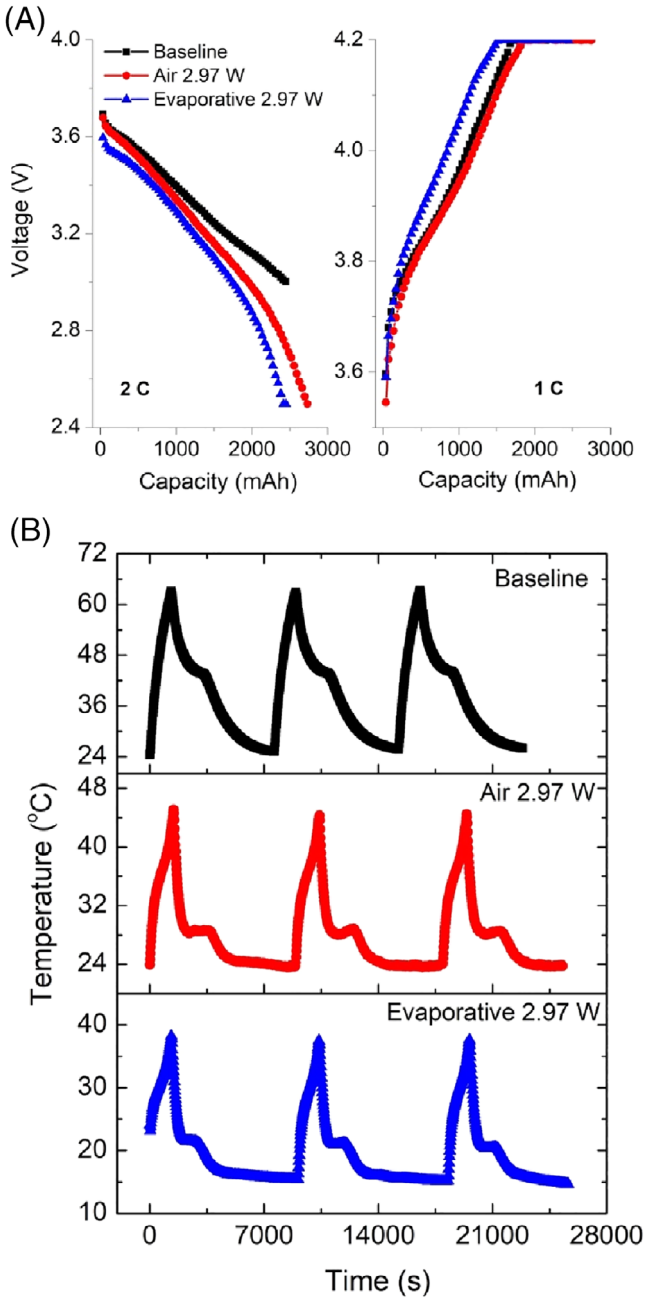


**FIGURE 6** A, Voltage (single cycle) and B, temperature (first three cycles) curves of the batteries cycled in different cooling conditions [Colour figure can be viewed at wileyonlinelibrary.com]

stage. The temperatures of the batteries drop after the flat plateaus since the charging current drops during the CV charging state. Among the batteries, the battery cycled in the baseline condition has the maximum temperature of 63.4°C, which is much higher than the temperatures of the batteries with the air cooling and DEC systems, with values of 45.1°C and 38.2°C, respectively.

Figure 7 shows the initial and final capacities as well as the capacity losses of the batteries cycled in these three cooling conditions. Prior to the cycle tests carried out in different cooling conditions, the batteries first underwent three cycles in the baseline condition to determine their initial capacities. It is seen that the batteries used for cycle tests in the baseline condition, air cooling condition, and DEC condition output initial capacities of 3197, 3170, and 3170 mAh, respectively.

The batteries were then cycled in three cooling conditions for 200 cycles. To clearly compare the capacity changes of the batteries cycled in different cooling conditions during the 200 cycles, the subtractions of their initial capacities from their capacities in the current cycle are plotted. Interestingly, the battery cycled in the baseline condition has smaller capacity drops than the other two batteries during the 200 cycles, though its operating temperature exceeds the suggested upper limit of 60°C. A possible explanation is that at a higher operating temperature, the capacity loss of the battery cycled in the baseline condition is closer to the real capacity loss, while the capacity losses of the batteries cycled in the air cooling and DEC conditions are enlarged due to the sensitivity of discharged capacity to the operating temperature. Fluctuations of the discharged capacities of the battery cycled in the DEC tunnel are also observed, which is due to the variations of the inlet air temperature caused by the RH changes during the cycle test.

Lastly, these three batteries underwent another three cycles in the baseline condition after the 200 cycles to determine their final capacities and the real capacity losses. As shown in Figure 7, the baseline battery has the highest capacity loss of 206 mAh among the tested batteries, followed by the battery cycled in air cooling condition and the battery in DEC condition, with capacities losses of 198 and 183 mAh, respectively.

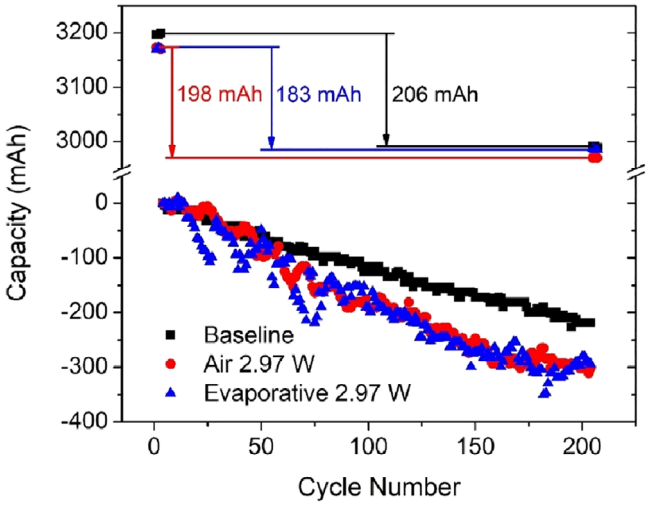


**FIGURE 7** Capacity fading plots of the batteries cycled in different cooling conditions [Colour figure can be viewed at wileyonlinelibrary.com]

## 3.4 | Cooling tests on a battery pack

After analyses of the DEC design on single batteries, cooling tests are then performed on a 9-cell battery pack. During the tests in ambient condition, the battery pack discharged capacities of 3250 and 3125 mAh at the discharge currents of 3 and 5 A, respectively. Figure 8A shows the recorded battery temperature at the assigned locations in the baseline condition. It is seen that location 3 has the highest temperature for both the 3 and 5 A discharges, which is ascribed to the heat accumulation and insufficient cooling at the battery pack center. The maximum temperature reaches 57.7°C during the 3 A discharge and exceeds 80°C at 5 A, far exceeds the allowable limit of 60°C for discharging. A higher temperature is expected in the center of batteries than the surface due to the low thermal conductivity in the radial direction of batteries.[33,34] In this regard, the battery pack will be dangerous to operate without a thermal management system even at the relatively low discharge current of 3 A. Effective cooling is indispensable for the battery pack for safe operations.

A study conducted by Pesaran et al[35] showed that the temperature difference inside a battery pack should be within 5°C, since big temperature differences can lead to uneven capacity fading and unbalanced charge and discharge between batteries.[36] Figure 8B shows the recorded maximum temperature differences of the battery pack during the 3 A and 5 A discharges in the baseline condition. The temperature differences increase with the discharges and decrease during the cooling period. The surface temperature of the interior battery (location 3) is 8.1°C and 14.8°C higher than the battery in the corner (location 2) during the 3 and 5 A discharges, respectively.

To alleviate the heat accumulation and improve the temperature uniformity, cooling tests were then carried out on the battery pack equipped with the air cooling and DEC systems during the 3 A discharges. During the tests, location 6 had the lowest temperature, while the highest temperature was found at location 1 because the cooling

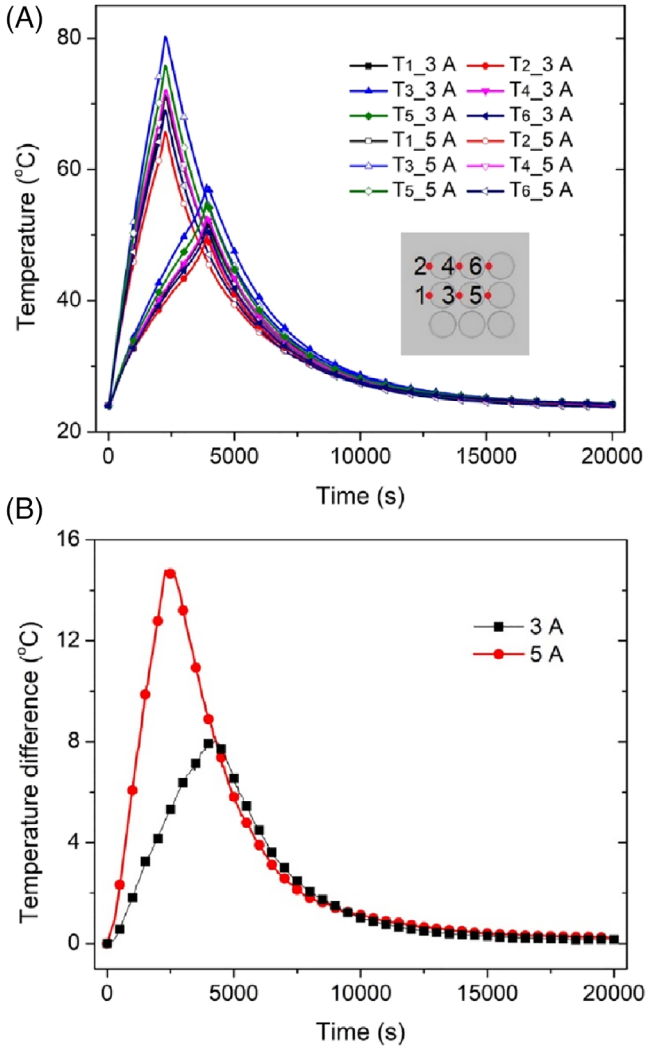


**FIGURE 8** A, Temperature at selected locations, and B, recorded maximum temperature differences in the battery pack during 3 A and 5 A discharges in the baseline condition [Colour figure can be viewed at wileyonlinelibrary.com]

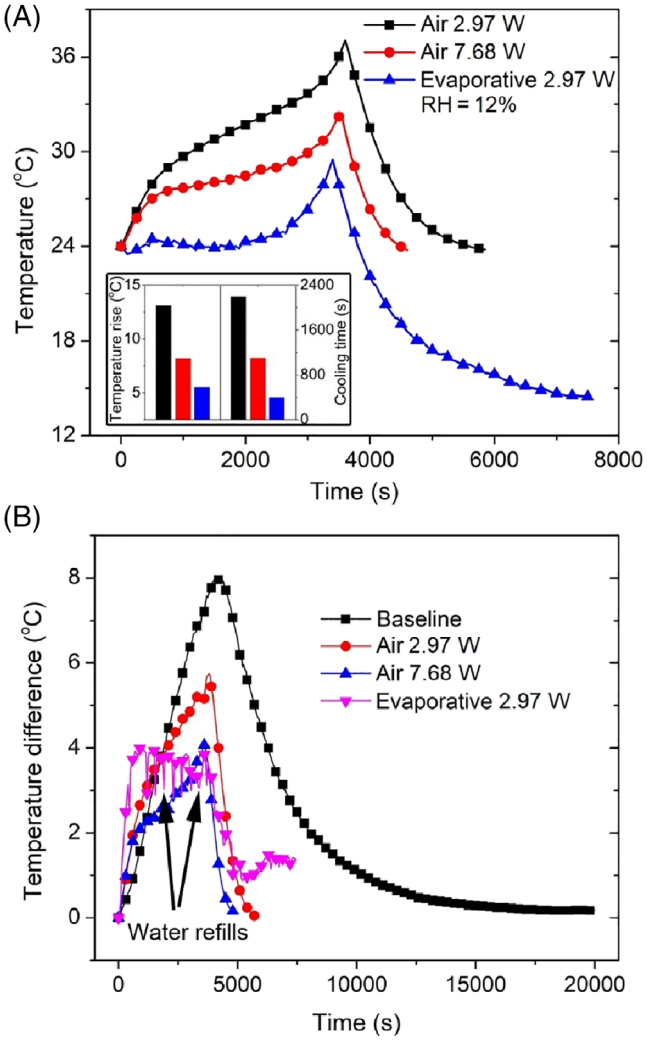


**FIGURE 9** Test results of the battery pack during 3 A discharges. A, The maximum temperature curves of the battery pack discharged in the air cooling and DEC tunnels. Inset: comparisons of the temperature rise and cooling time of the battery pack equipped with the air cooling and DEC systems. B, The maximum temperature difference curves of the battery pack discharged in different cooling conditions [Colour figure can be viewed at wileyonlinelibrary.com]

air was heated as it passed the batteries. For a clear comparison, the maximum temperature curves ($T_1$) and the maximum temperature difference curves ($T_1$–$T_6$) are plotted in Figure 9A,B, respectively. It is seen that the forced cooling systems can effectively manage the temperature and temperature difference of the battery pack at low levels. For the air cooling, the maximum temperature inside the battery pack is 37.1°C when the fan operates at 2.97 W, and it drops to 32.2°C as the fan power increases to 7.68 W; the temperature difference in the pack exceeds the recommended 5°C and peaks at 5.7°C at a fan power of 2.7 W, and it drops to 4.1°C when the fan operates at 7.68 W.

The DEC tunnel shows better cooling performance. Even at a low input power of 2.97 W, the tunnel can manage the maximum temperature and temperature difference of the battery pack within 30°C and 4°C, respectively. It is also seen that the temperature difference drops after each water refill. This is because the injection of room temperature water breaks the balance of evaporation and increase the inlet air temperature. The batteries in the first row is more sensitive to this change and experience slight temperature jumps, which as a result increases the temperature at location 6 and reduces the value of $T_1$–$T_6$. In addition, the maximum temperature rises and cooling times of the battery pack during the 3 A discharges are plotted in a column chart in the inset of

Figure 9A. It is seen that the battery pack equipped with the DEC system has a significantly lower temperature rise and shorter cooling time than the battery pack equipped with the air cooling system.

In Figure 10A, the maximum temperature curves of the battery pack equipped with the air cooling and DEC systems during the 5 A discharges are plotted. Although the maximum temperature of the battery pack equipped with forced air cooling system is significantly lower than that of the baseline condition, it still exceeds 50°C when the fan operates at a power of 2.97 W. The maximum temperature drops with the increase of the fan power, and a temperature of 40.3°C is obtained when the fan operates at 12.0 W. In comparison, the DEC system shows better cooling capability. The maximum temperatures are 40.4°C, 35.2°C, and 33.6°C at input powers of 2.97, 7.68, and 12.0 W, respectively.

Figure 10B summarizes the maximum temperature rises and differences of the battery pack during 5 A discharges. With the forced air cooling, the maximum temperature differences of the battery pack are 11.4°C, 9.6°C, and 6.9°C at fan powers of 2.97, 7.68, and 12.0 W, respectively. Though relatively lower temperature differences are achieved in the DEC tunnel, they are above the recommended maximum temperature difference of 5°C inside battery packs.

Reciprocating air flow can redistribute the heat and disturb the pre-formed boundary layer, thus alleviating the heat accumulation and improving the temperature uniformity. In Reference 26, the reciprocating air flow has been numerically studied on a forced air cooling system, and a switching period of 120 seconds was found to be optimum and is used in this work on the DEC tunnel. In Figure 11A,B, the temperatures and

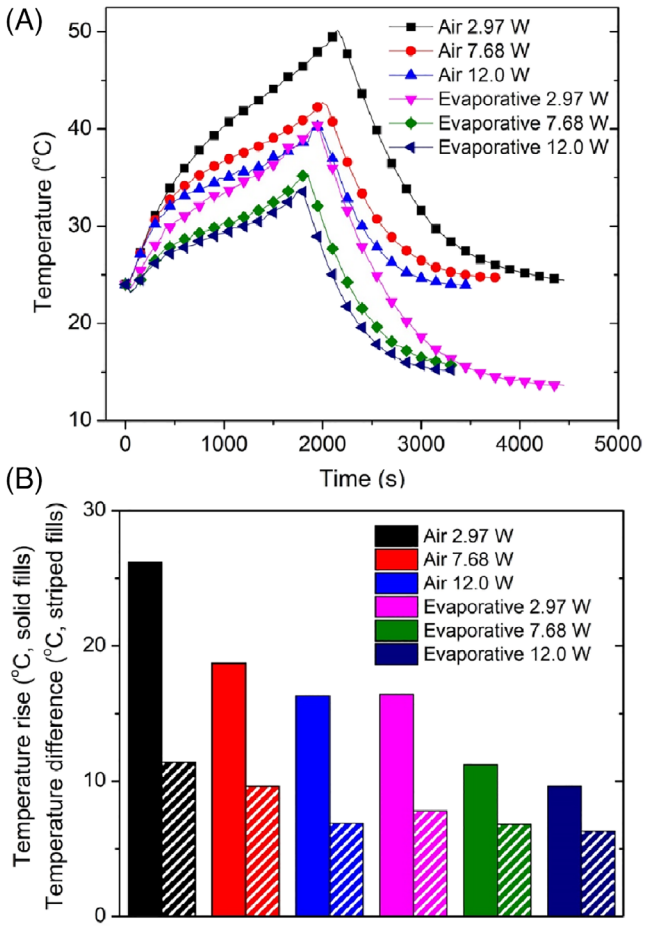


**FIGURE 10** Test results of the battery pack during 5 A discharges. A, The maximum temperature curves of the battery pack discharged in air cooling and DEC tunnels. B, comparisons of the temperature rise and maximum temperature difference of the battery pack equipped with air cooling and DEC systems [Colour figure can be viewed at wileyonlinelibrary.com]

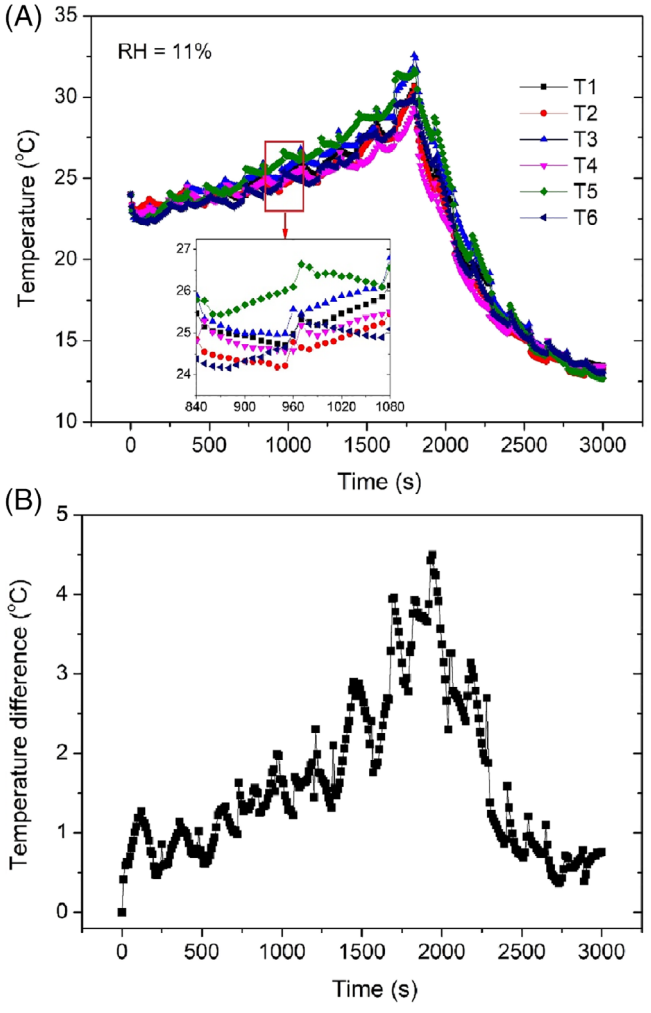


**FIGURE 11** A, Temperature and B, temperature difference curve of the battery pack during a 5 A discharge in a DEC tunnel with the reciprocating air flow [Colour figure can be viewed at wileyonlinelibrary.com]

**TABLE 4** Summary of the cooling results of the battery pack

| | 3 A | | 5 A | |
|---|---|---|---|---|
| | $T_{max}$ (°C) | $\Delta T_{max}$ (°C) | $T_{max}$ (°C) | $\Delta T_{max}$ (°C) |
| Baseline | 56.7 | 8.1 | 79.2 | 14.8 |
| 9 V direct | 36.1 | 5.7 | 49.2 | 11.4 |
| 12 V direct | 31.2 | 4.1 | 41.7 | 9.6 |
| 15 V direct | — | — | 39.3 | 6.9 |
| 9 V EC | 28.5 | 3.9 | 39.4 | 7.8 |
| 12 V EC | — | — | 34.2 | 6.5 |
| 15 V EC | — | — | 32.6 | 6.3 |
| 12 V ECR | — | — | 32.6 | 4.5 |

Abbreviations: EC, evaporative cooling; ECR, evaporative cooling with the reciprocating air flow.

temperature differences of the battery pack during a 5 A discharge are plotted, in which the cooling fans were operated at a power of 7.68 W. It is seen that after employing the reciprocating cooling strategy, the maximum recorded temperature shifts from the downstream battery to the interior battery, with its value dropping to 32.6°C. As the zoomed inset shown in Figure 11A, by reversing the direction of air flow periodically, the batteries on the left and right ends are alternatively cooled, which effectively alleviates the formation of hot air on any side. Therefore, the temperature difference in the battery pack is kept at a lower level compared to the one-directional cooling tunnel, with a maximum value of 4.5°C, as seen in Figure 11B. A summary of the cooling results of the battery pack is given in Table 4.

## 4 | CONCLUSION

In this paper, a DEC approach is introduced and studied for Li-ion battery thermal management. Cooling experiments were carried on both single batteries and battery pack in cooling tunnels that can produce one-directional and reciprocating air flows. Three cooling conditions including natural convection cooling (baseline), forced air cooling and DEC were compared on their ability in lowering the temperature rise and reducing the capacity loss of batteries.

In the baseline condition, both the individual battery and battery pack experienced dramatic temperature increases, and it is noteworthy that the temperature and temperature difference of the battery pack even peak at 80.2°C and 14.8°C during a 5 A discharge. With equipping the forced air cooling systems, significantly lower temperatures and temperature differences were achieved. The DEC showed a further enhanced cooling performance compared to the air cooling due to the lower intake air temperatures, which was achieved by the absorption of the sensible heat of air during the water evaporation process.

A comprehensive study of the DEC showed that the cooling performance of DEC is closely related to the RH of the ambient air, and a low RH is preferred for better cooling effects. In addition, an analysis of the psychrometric chat showed that the DEC is more robust for applications with higher ambient temperatures due to the increased CP, thereby expanding the usage of Li-ion batteries in more adverse and intensive operating conditions. A comparison between the DEC and air cooling revealed that the DEC can achieve better cooling effects than the air cooling even at a lower fan power, thus reducing the power consumption and fan noise. Cycle test results indicated that the battery equipped with the DEC has improved long-term performance, with a less capacity loss than the batteries cycled in baseline and air cooling conditions.

Lastly, a DEC tunnel with a reciprocating air flow mode was built to improve the temperature uniformity in the battery pack, since both the one-directional air cooling and DEC systems were failed to maintain the maximum temperature difference of the battery pack in the recommended range of 5°C due to the heat accumulation in the downstream passages. The reciprocating air flow periodically redistributed the heat in the battery pack and achieved a lower maximum temperature difference of 4.5°C.

## ACKNOWLEDGEMENTS

Dr Zhao sincerely thank the fellowship from the National Sciences and Engineering Research Council (NSERC) of Canada and Carleton University. The funding support

from Chongqing Technology and Business University (Fund No.: KFJJ2016034) is also appreciated.

## NOMENCLATURE

$A$ area ($m^2$)
$h$ convective heat transfer coefficient ($W/m^2/K$)
$\dot{Q}$ heat dissipation rate (W)
$T_f$ temperature of cooling medium (K)
$T_s$ temperature of battery surface (K)
$\Delta T$ temperature drop due to evaporation cooling (K)

## ORCID

*Jie Liu* https://orcid.org/0000-0001-7493-0882

## REFERENCES

1. Kabir MM, Demirocak DE. Degradation mechanisms in Li-ion batteries: a state-of-the-art review. *Int J Energy Res*. 2017;41:1963-1986.
2. Hao M, Li J, Park S, Moura S, Dames C. Efficient thermal management of Li-ion batteries with a passive interfacial thermal regulator based on a memory alloy. *Nat Energy*. 2018;3:899-906.
3. Zhao R, Zhang S, Liu J, Gu J. A review of thermal performance improving methods of lithium ion battery: Electrode modification and thermal management system. *J Power Sources*. 2015;299:557-577.
4. Al-Zareer M, Dincer I, Rosen MA. A review of novel thermal management systems for batteries. *Int J Energy Res*. 2018;42:3482-3205.
5. He F, Li X, Zhang G, Zhong G, He J. Experimental investigation of thermal management system for lithium ion batteries module with coupling effect by heat sheets and phase change materials. *Int J Energy Res*. 2018;42:3279-3288.
6. Zhao R, Gu J, Liu J. Optimization of a phase change material based internal cooling system for cylindrical Li-ion battery pack and a hybrid cooling design. *Energy*. 2017;135:811-822.
7. Al-Zareer M, Dincer I, Rosen MA. A novel phase change based cooling system for prismatic lithium ion batteries. *Int J Refrig*. 2018;86:203-217.
8. Zhao R, Gu J, Liu J. Performance assessment of a passive core cooling design for cylindrical lithium-ion batteries. *Int J Energy Res*. 2018;42:2728-2740.
9. Zou D et al. Preparation of a novel composite phase change material (PCM) and its locally enhanced heat transfer for power battery module. *Energ Conver Manage*. 2019;180:1196-1202.
10. Ling Z, Wen X, Zhang Z, Fang X, Gao X. Thermal management performance of phase change materials with different thermal conductivities for Li-ion battery packs operated at low temperatures. *Energy*. 2018;144:977-983.
11. Zhao R, Zhang S, Gu J, Liu J, Carkner S, Lanoue E. An experimental study of lithium ion battery thermal management using flexible hydrogel films. *J Power Sources*. 2014;255:29-36.
12. Ren Y, Yu Z, Song G. Thermal management of a Li-ion battery pack employing water evaporation. *J Power Sources*. 2017;360:166-171.
13. Zhang S, Zhao R, Liu J, Gu J. Investigation on a hydrogel based passive thermal management system for lithium ion batteries. *Energy*. 2014;68:854-861.
14. Hirano H, Tajima T, Hasegawa T, Sekiguchi T, Uchino M. Boiling liquid battery cooling for electric vehicle. In Proceedings of Transportation Electrification Asia-Pacific. 2014. Beijing.
15. An Z, Jia L, Li X, Ding Y. Experimental investigation on lithium-ion battery thermal management based on flow boiling in mini-channel. *Appl Therm Eng*. 2017;117:534-543.
16. van Gils RW, Danilov D, Notten PHL, Speetjens MFM, Nijmeijer H. Battery thermal management by boiling heat-transfer. *Energ Conver Manage*. 2014;79:9-17.
17. Shah K, Drake SJ, Wetz DA, et al. Modeling of steady-state convective cooling of cylindrical Li-ion cells. *J Power Sources*. 2014;258:374-381.
18. Mo X, Hu X, Tang J, Tian H. A comprehensive investigation on thermal management of large-capacity pouch cell using micro heat pipe array. *Int J Energy Res*. 2019;43:7444-7458.
19. Shahid S, Agelin-Chaab M. Experimental and numerical studies on air cooling and temperature uniformity in a battery pack. *Int J Energy Res*. 2018;42:2246-2262.
20. Lu Z, Yu X, Wei L, et al. Parametric study of forced air cooling strategy for lithium-ion battery pack with staggered arrangement. *Appl Therm Eng*. 2018;136:28-40.
21. Park H. A design of air flow configuration for cooling lithium ion battery in hybrid electric vehicles. *J Power Sources*. 2013;239:30-36.
22. Li X, He F, Ma L. Thermal management of cylindrical batteries investigated using wind tunnel testing and computational fluid dynamics simulation. *J Power Sources*. 2013;238:395-402.
23. Yang N, Zhang X, Li G, Hua D. Assessment of the forced air-cooling performance for cylindrical lithium ion battery packs: a comparative analysis between aligned and staggered cell arrangements. *Appl Therm Eng*. 2015;80:55-65.
24. Wang T, Tseng KJ, Zhao J, Wei Z. Thermal investigation of lithium-ion battery module with different cell arrangement structures and forced air cooling strategies. *Appl Energy*. 2014;134:229-238.
25. Sun H, Dixon R. Development of cooling strategy for an air cooled lithium-ion battery pack. *J Power Sources*. 2014;272:404-414.
26. Mahamud R, Park C. Reciprocating air flow for Li-ion battery thermal management to improve temperature uniformity. *J Power Sources*. 2011;196:5685-5696.
27. Sun Y, Guan Z, Gurgenci H, Wang J, Dong P, Hooman K. Spray cooling system design and optimization for cooling performance enhancement of natural draft dry cooling tower in concentrated solar power plants. *Energy*. 2019;168:273-284.
28. Farzaneh-Gord M, Deymi-Dashtebayaz M. Effect of various inlet air cooling methods on gas turbine performance. *Energy*. 2011;36:1196-1205.
29. Carmona J. Gas turbine evaporative cooling evaluation for Lagos – Nigeria. *Appl Therm Eng*. 2015;89:262-269.
30. Zhao R, Gu J, Liu J. An experimental study of heat pipe thermal management system with wet cooling method for lithium ion batteries. *J Power Sources*. 2015;273:1089-1097.
31. https://www.weathercentral.com/weather/us/index.html. US weather - national relative humidity map. Accessed August 28, 2019.
32. Chen X, Su Y, Aydin D, et al. A novel evaporative cooling system with a polymer hollow fibre spindle. *Appl Therm Eng*. 2018;132:665-675.
33. Zhang G, Cao L, Ge S, Wang CY, Shaffer CE, Rahn CD. In situ measurement of radial temperature distributions in cylindrical Li-ion cells. *J Electrochem Soc*. 2014;161:A1499-A1507.

34. Anthony D, Wong D, Wetz D, Jain A. Non-invasive measurement of internal temperature of a cylindrical Li-ion cell during high-rate discharge. *Int J Heat Mass Transf*. 2017;111:223-231.
35. Pesaran AA. Battery thermal models for hybrid vehicle simulations. *J Power Sources*. 2002;110:377-382.
36. Yang N, Zhang X, Shang B, Li G. Unbalanced discharging and aging due to temperature differences among the cells in a lithium-ion battery pack with parallel combination. *J Power Sources*. 2016; 306:733-741.

**How to cite this article:** Zhao R, Liu J, Gu J, Zhai L, Ma F. Experimental study of a direct evaporative cooling approach for Li-ion battery thermal management. *Int J Energy Res*. 2020;44: 6660–6673. https://doi.org/10.1002/er.5402